

Selected Papers from the 3rd Radiocarbon in the Environment Conference, Gliwice, Poland, 5–9 July 2021  
© The Author(s), 2023. Published by Cambridge University Press for the Arizona Board of Regents on behalf of the University of Arizona. This is an Open Access article, distributed under the terms of the Creative Commons Attribution licence (<http://creativecommons.org/licenses/by/4.0/>), which permits unrestricted re-use, distribution and reproduction, provided the original article is properly cited.

## LINKING RADIOCARBON AND TROPHIC WEBS IN KARSTIC GROUNDWATER ECOSYSTEMS IN THE YUCATAN PENINSULA, MÉXICO

C Solís<sup>1</sup>  • E M Chávez-Solís<sup>2,3,4\*</sup> • M Rodríguez-Ceja<sup>1</sup> • C G Méndez-García<sup>1</sup> • E Ortiz<sup>5</sup> • C Canto<sup>6</sup> • M A Martínez-Carrillo<sup>7</sup>  • M Mascaró<sup>3</sup>

<sup>1</sup>Instituto de Física, Universidad Nacional Autónoma de México (UNAM), Ave. Universidad 3000. 04510, Cd. de México, Mexico

<sup>2</sup>Posgrado en Ciencias Biológicas, Unidad de Posgrado Edificio A, 1 er piso Circuito de Posgrado, Ciudad Universitaria, Universidad Nacional Autónoma de México, 04510, México City, México

<sup>3</sup>Unidad Multidisciplinaria de Docencia e Investigación Sisal, Facultad de Ciencias, Universidad Nacional Autónoma de México, Puerto de Abrigo s/n, 97356, Sisal, Yucatán, México

<sup>4</sup>Instituto de Investigaciones Oceanológicas, Universidad Autónoma de Baja California, Carretera Ensenada-Tijuana No. 3917, Fracc. Playitas, 22860, Ensenada, Baja California, México

<sup>5</sup>Área de Química y Fisicoquímica Ambiental, Universidad Autónoma Metropolitana, Azcapotzalco, México City, México

<sup>6</sup>Tecnológico de Monterrey, Escuela de Ingeniería y Ciencias, Calle Puente 222, Coapa, Arboledas del Sur, Tlalpan, 14380, México City, México

<sup>7</sup>Facultad de Ciencias. Universidad Nacional Autónoma de México. Circuito de la Investigación Científica S/N. Ciudad Universitaria. 04510, México City, México

**ABSTRACT.** Stable isotopes have been used historically to track food webs. Our approach used a combination of  $\delta^{13}\text{C}$  and radiocarbon ( $^{14}\text{C}$ ) dating to identify carbon sources in cave shrimp within caves of the Karstic Yucatan Peninsula, Mexico. Three sister species of stygobitic *Typhlatya* shrimps were collected from the cenote pool (cenote hereafter), cavern and cave hydro regions. New and previously reported  $^{14}\text{C}$  and  $\delta^{13}\text{C}$  values of whole tissues from the organisms were determined at the AMS laboratory (LEMA) of the Institute of Physics of the Universidad Nacional Autónoma de México. This new set of isotopic values of biomass and potential sources were incorporated into the Bayesian Mixing Modeling Software *SIAR*. In two hypothetical scenarios, the contribution from each feeding source among three species of the *Typhlatya* genus was determined. Slight differences were also observed between isotopic values of two groups of the same species collected in two distant cenote pools, suggesting this species may feed on a wider array of sources than previously found, and that the oligotrophic environment may have a strong influence on cave shrimp diet.

**KEYWORDS:** anchialine, radiocarbon AMS, *Typhlatya*, Yucatan Peninsula.

## INTRODUCTION

The geology of Yucatan, Mexico, is composed of carbonate and evaporite rocks, forming a karst platform. In this region, there are no rivers; rainwater quickly seeps down to the aquifer. Thus, the primary geochemical process in karst aquifers is the dissolution of carbonate rocks, leaving little residue and a thin or almost non-existent ground cover. As a result, a geological feature of the Yucatan Peninsula is a great density of sinkholes, locally known as cenotes, which give way to large dissolution caves and underground cavities, some of which are linked together in a complex geomorphological structure.

In the Yucatan Peninsula, water of meteoric origin infiltrates and accumulates in the subsoil, forming a freshwater lens that floats on a denser mass of saline water, the origin of which is a marine intrusion through the permeable karstic rock. This vertical stratification is found in coastal systems also known as anchialine systems or subterranean estuaries and has major ecological implications for the cave biodiversity of Yucatan. Although marine intrusion may be found deeper in cenotes that are further from the coast, most cenotes in Yucatan State are exclusively freshwater.

\*Corresponding author. Email: [chavezsolis.efrain@gmail.com](mailto:chavezsolis.efrain@gmail.com)

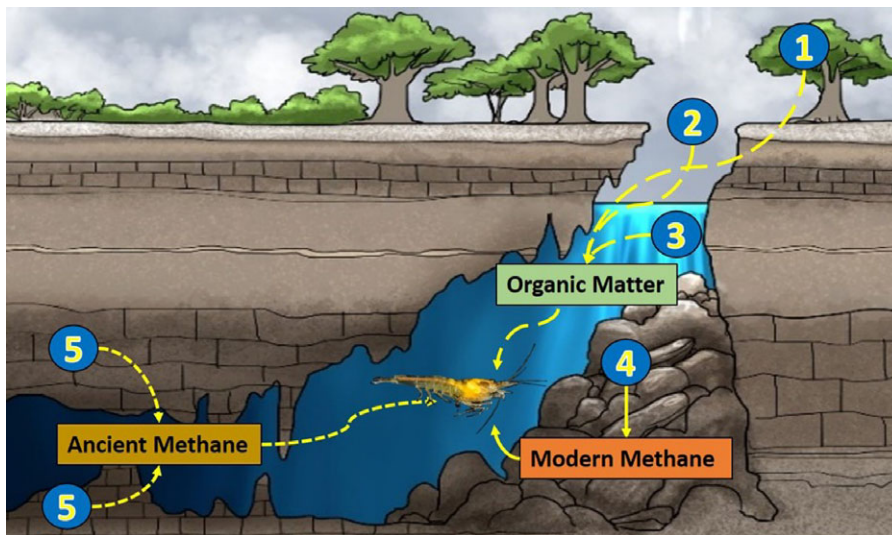


Figure 1 Conceptual framework of radiocarbon uptake by crustaceans in karstic groundwater: (1) Allochthonous photosynthetic matter; (2) atmospheric CO<sub>2</sub> that is permeated into the water table; (3) *in situ* photosynthesis in the cenote; (4) methane produced from modern sediments and organic matter; (5) radiocarbon-dead carbon which is biosynthesized.

*Typhlatya* species are found throughout marine and fresh groundwater habitats and are some of the most abundant and widespread stygofauna in the anchialine ecosystems of the Yucatan Peninsula (Chávez-Solís et al. 2020). These crustaceans, of the Atyidae family, are a fundamental part of the food web of anchialine systems, as they feed on bacteria and organic material deposited within the aquifer and transfer energy to higher trophic levels. Figure 1 shows a conceptual framework of radiocarbon (<sup>14</sup>C) uptake in karstic groundwater fauna.

The isotopic signature has been widely used to identify chemical compounds, origin, flux, and transformation in biological and environmental systems. The stable and radioactive isotopes have the same chemical properties of their respective elements but can be distinguished with proper analytical techniques. Carbon isotopes (<sup>12</sup>C, <sup>13</sup>C, and <sup>14</sup>C; expressed as δ<sup>13</sup>C and Δ<sup>14</sup>C) are commonly used for studying food webs. To identify the carbon sources among ecologically similar species within anchialine systems, the use of δ<sup>13</sup>C is complemented, with the amount of radiocarbon, as such abundance reflects the modern or old character of the carbon sources. Organic tissues, dissolved organic carbon (DOC), and dissolved inorganic carbon (DIC) contained in the water show values of relative abundancies that can vary from Δ<sup>14</sup>C = –1000‰ for old carbon, to over +400‰ for modern carbon, offering a greater resolution, compared with δ<sup>13</sup>C sources (McCallister et al. 2004). These parameters provide an opportunity to better understand the role of potential food sources for the *Typhlatya* genus and the food web dynamics in cenotes.

In this work, we analyzed the <sup>13</sup>C and <sup>14</sup>C composition of 4 new, and 13 previously-published samples of the *Typhlatya* genus (Chávez-Solís et al. 2020). The <sup>14</sup>C composition of DIC in water from 4 new cenotes located along the Yucatan Peninsula was also included (Table 1). Radiocarbon analysis was carried out at the AMS laboratory (LEMA) of the Institute of Physics of the National Autonomous University of Mexico. The three studied species of the

Table 1  $\delta^{13}\text{C}$  and  $\Delta^{14}\text{C}$  results of *Typhlatya* biomass and groundwater samples. Local laboratory code, sample identification, site of collection,  $\delta^{13}\text{C}$  obtained by AMS or IRMS in parentheses, the uncertainty of the  $\delta^{13}\text{C}$  measurement,  $\Delta^{14}\text{C}$  and its uncertainty, and the reference if previously published.

LEMA code	Sample	Site	$\delta^{13}\text{C}$ (‰) AMS (IRMS)	1 $\sigma$	$\Delta^{14}\text{C}$ (‰)	1 $\sigma$	Reference
1458	<i>T. mitchelli</i>	Tza Itza	-26.3	1.4	-3.5	3.5	Chávez-Solís et al. (2020)
1459	<i>T. mitchelli</i>	Tza Itza	-23.0 (-23.5)	2.3 (0.2)	-15.8	3.4	Chávez-Solís et al. (2020)
1460	<i>T. mitchelli</i>	Tza Itza	-25.5 (-25.7)	1.1 (0.2)	-6.8	4.0	Chávez-Solís et al. (2020)
1461	<i>T. mitchelli</i>	Tza Itza	-25.9 (-26.3)	0.8 (0.2)	-9.4	3.7	Chávez-Solís et al. (2020)
1462	<i>T. mitchelli</i>	Tza Itza	-26.0 (-26.2)	2.0 (0.2)	-9.2	3.7	Chávez-Solís et al. (2020)
1463	<i>T. mitchelli</i>	Tza Itza	-25.5	1.0	+19.2	3.7	Chávez-Solís et al. (2020)
1372	<i>T. pearsei</i>	Nohmozon	-41.0	1.5	-166.0	3.3	Chávez-Solís et al. (2020)
1374	<i>T. pearsei</i>	Nohmozon	-38.0	1.0	-202.0	3.5	Chávez-Solís et al. (2020)
1375	<i>T. pearsei</i>	Nohmozon	-35.0	1.0	-194.4	2.6	Chávez-Solís et al. (2020)
1097	<i>T. dzilamensis</i>	Xtabay	-43.7	0.7	-135.5	2.7	Chávez-Solís et al. (2020)
1099	<i>T. dzilamensis</i>	Xtabay	-42.0	0.4	-131.0	2.5	Chávez-Solís et al. (2020)
1130	<i>T. dzilamensis</i>	Xtabay	-34.0	0.6	-122.0	2.8	Chávez-Solís et al. (2020)
1131	<i>T. dzilamensis</i>	Xtabay	-31.0	0.3	-91.5	3.0	Chávez-Solís et al. (2020)
1980	<i>T. mitchelli</i>	Palomitas	-24.0	1.3	-56.1	2.9	This work
1981	<i>T. mitchelli</i>	Palomitas	-22.0	1.0	-56.3	2.8	This work
1982	<i>T. mitchelli</i>	Palomitas	-19.0	0.8	-57.2	3.0	This work
1983	<i>T. mitchelli</i>	Palomitas	-23.0	1.2	-60.2	3.0	This work
1356	FGW	Cholul	-14.4	0.7	-218.6	2.6	This work
1357	FGW	Cholul	-16.4	0.6	-219.3	2.9	This work
1358	FGW	Xoch	-16.8	0.6	-296.5	2.2	This work
1436	FGW	Xlakah	-16.4	0.9	-289.6	2.2	This work
1371	FGW	Nohmozon	-16.1	0.8	-247.0	3.0	Chávez-Solís et al. (2020)
1467	FGW	Tza Itza	-10.8	1.8	-203.0	3.0	Chávez-Solís et al. (2020)
1156	FGW	Xtabay	-10.3	1.5	-184.7	3.0	Chávez-Solís et al. (2020)
1155	SGW	Xtabay	-13.6	0.7	-252.6	2.8	Chávez-Solís et al. (2020)

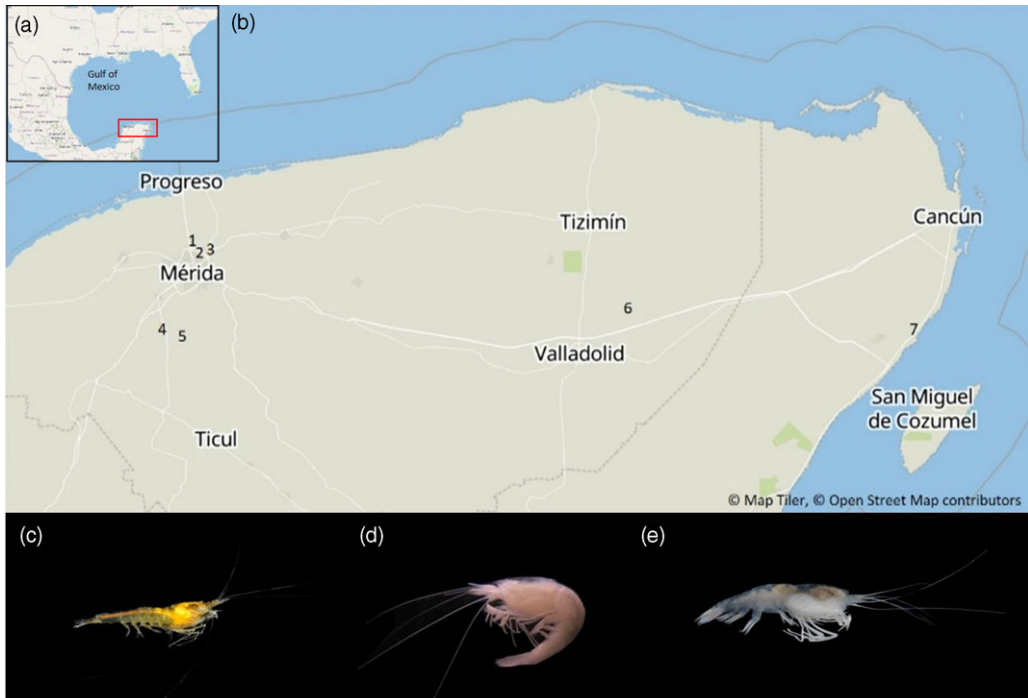


Figure 2 (a) Location of the Yucatan Peninsula within the Gulf of Mexico. (b) Location of sampling sites of *Typhlatya* specimens and groundwater in the Yucatan Peninsula; cenote Xlakah in dzibilchaltun (1); cenote Xoc (2) and a well from Cholul (3), in Mérida; Tza Itza (4) and Nohmozon (5) in Tecoh; Palomitas (6) in Yalcobá; and Xtabay (7) in Puerto Aventuras. (c) *T. mitchelli*. (d) *T. pearsei*. (e) *T. dzilamensis*. Photo credits: (c): Benjamin Magaña, (d) and (e): EC.

genus *Typhlatya*: *T. mitchelli*, *T. dzilamensis* and *T. pearsei* (Figure 2b–d), are endemic to the Yucatan Peninsula. Furthermore, *T. mitchelli* and *T. pearsei* are under the “special protection” of endangered categories in the local regulation NOM-059-SEMARNAT.

Although these species have been observed to share parts of the subterranean habitat, Benítez et al. (2019) and Chávez-Solís et al. (2020) showed that the distribution of these species in these particular habitats is not random; *T. pearsei* is found in the freshwater pools of the cenote, where sunlight allows for in situ photosynthesis and allochthonous input is greatest. *T. mitchelli* is found in freshwater, mainly in the caverns close to the cenote pools, where allochthonous and photosynthesis derived matter is transported from the cenote towards the cavern. Finally, *T. dzilamensis* inhabits saline groundwater inside the caves, where allochthonous matter is scarce.

The isotopic values of *Typhlatya* biomass published in Chávez-Solís et al. (2020) were incorporated to new biomass samples along with potential carbon sources and were analyzed with Bayesian mixture modeling software SIAR (version 4.2) (Parnell and Jackson 2013).

We sought to identify different feeding sources among three species of the *Typhlatya* genus using isotopic values of potential sources and as biomass adding a new site with different

environmental characteristics for *T. mitchelli* using values of  $^{14}\text{C}$  and  $^{13}\text{C}$  abundances obtained by AMS, into the Bayesian Mixing Modeling Software *SIAR*.

## MATERIALS AND METHODS

### Sample Collection and Habitat

We examined  $^{13}\text{C}$  and  $^{14}\text{C}$  composition of 4 new and 13 previously published biomass samples of *Typhlatya* individuals. The new set consisted of *T. mitchelli* samples collected under the sulfur cloud in cenote Palomitas (Figure 2). This cenote pool is characterized by the presence of a sulfur cloud at 45 m deep.

Water samples from cenotes Palomitas (20.819N, -88.055W), Xlakah (21.090N, -89.598W), Xoc (21.032N, -89.577W), and a well from Cholul (21.047N, -89.553W), were sampled to explore the variation range of  $^{14}\text{C}$  within DIC in groundwater of the Yucatan Peninsula (Figure 2). Two replicates were collected in 50 mL falcon tubes and stored at cold temperature in the dark until analysis.

As previously reported in Chavez-Solis et al. (2020), the *Typhlatya* species were found in different zones within the anchialine ecosystem: *T. pearsei* was predominantly found at night in the cenote pool, which is directly under the surface and has the greatest interaction with external factors, may have sunlight incidence, and is the entrance of external input; *T. mitchelli* in the cavern area, a transitional zone between the cenote pool and the cave, with a moderate amount of light (twilight zone), and *T. dzilamensis* in the cave where sunlight never reaches. Five *T. mitchelli* from the cavern of cenote Tza Itza were collected at 13 m of depth (Chávez-Solis et al. 2020), while four *T. mitchelli* from the cavern of cenote Palomitas were collected at 45 m of depth (new data), just below a sulfur cloud; three *T. pearsei* were collected from the cenote pool of Nohmozon at 16 m of depth (Chávez-Solis et al. 2020), only 20 km southeast from Tza Itza, and Five *T. dzilamensis* (Chávez-Solis et al. 2020) were collected from ponderosa system in cave passages adjacent to Xtabay cenote below the halocline at 14 m depth (Figure 2).

### Sample Preparation and AMS Analysis

After collection, the *Typhlatya* samples were rinsed with distilled water and dried at 60°C. For AMS analyses, samples underwent a cleansing with ultrapure water and a chemical treatment using the acid-base-acid (ABA) protocol, to remove salts and other adhered contaminants. Cleaned samples were processed in automated graphitization equipment (AGE III from Ion Plus). The sample (~1 mg C) was combusted at 950°C in an Elemental Analyzer and the  $\text{CO}_2$  produced was transferred to a reactor where it reacted with hydrogen in the presence of iron powder to produce pure graphite. Oxalic acid II (NIST SRM 4990C) was used as a primary standard, and phthalic anhydride (without  $^{14}\text{C}$ ) was used as a blank. The graphite analysis of  $^{14}\text{C}$ ,  $^{13}\text{C}$ , and  $^{12}\text{C}$  abundance was performed in a 1 MV accelerator mass spectrometry (AMS) system High Voltage Europe Engineering (HVEE) at the Laboratorio Nacional de Espectrometría de Masas (LEMA) of the Institute of Physics, Universidad Nacional Autónoma de México (UNAM) in Mexico City.

Relative abundance of  $^{13}\text{C}$  and  $^{12}\text{C}$  isotopes in a sample can be reported in delta notation ( $\delta$ ), calculated using the following equation:

$$\delta^{13}\text{C} = \left[ \left( \frac{^{13}\text{C}/^{12}\text{C}_{\text{sample}}}{^{13}\text{C}/^{12}\text{C}_{\text{standard}}} - 1 \right) / \left( \frac{^{13}\text{C}/^{12}\text{C}_{\text{standard}}}{^{13}\text{C}/^{12}\text{C}_{\text{standard}}} \right) \right] \times 1000 \quad (1)$$

Relative abundance of  $^{14}\text{C}$  and  $^{12}\text{C}$  can be expressed by  $\Delta^{14}\text{C}$ , the  $^{14}\text{C}$  isotopic ratio of a material relative to the modern standard after correction for fractionation to  $\delta^{13}\text{C} = -25\text{‰}$ :

$$\Delta^{14}\text{C} = 1000 \left[ \text{fm} e^{(0.00012 \cdot (1950 - x))} - 1 \right]$$

where fm is the fraction of modern  $^{14}\text{C}$  corrected for isotopic fractionation by use of  $\delta^{13}\text{C}$ , and x is the year of deposition (determined from the  $^{210}\text{Pb}$  chronology) (Stuiver and Polach 1977).

The measured  $^{14}\text{C}/^{12}\text{C}$  isotopic ratios were corrected for isotopic fractionation using the  $^{13}\text{C}/^{12}\text{C}$  isotopic ratios measured in the accelerator. Corresponding radiocarbon ages were calculated using computer codes developed at LEMA.

Due to the protected category and the small biomass ( $\sim 0.03$  gr) of *Typhlatya* individuals, this study could only sample a small number of individuals, hence the  $\delta^{13}\text{C}$  of only a few samples was analyzed by both AMS and IRMS (Table 1). The AMS  $\delta^{13}\text{C}$  obtained values were in an excellent approximation to the values obtained by isotope ratio mass spectrometry (IRMS) performed at the Laboratory of Stable Isotope Analyses at the Scientific and Technological Park of Yucatan (PCYT, UNAM) (Table 1). Therefore, we used the  $\delta^{13}\text{C}$  values obtained by AMS for the rest of the samples and assumed they were reliable indicators in the analyses of food sources in *Typhlatya* biomass contribution (Prasad et al. 2019).

We obtained  $\text{CO}_2$  from DIC in water samples by hydrolysis with 85% orthophosphoric acid in a precleaned flask flushed with helium. The obtained  $\text{CO}_2$  was then transferred to AGEIII to obtain graphite by bubbling helium gas through the sample. We also processed IAEA-C1 (Marble) and C2 (Travertine) standards in water by acid hydrolysis. The results of the isotopic concentrations are shown in Figure 3, where the values of  $\delta^{13}\text{C}$  for each specimen are plotted against the respective values of  $\Delta^{14}\text{C}$ , the values for the fresh groundwater (FGW) and saline groundwater (SGW) for the different sites are also indicated.

### Mixing Model Analysis

To explain if the lower  $\Delta^{14}\text{C}$  values of *T. mitchelli* from Palomitas can be linked to a different carbon source than those from Tza Itza, we combined this new group with the previously obtained results into a Bayesian mixing model (Parnell and Jackson 2013). This approach allows flexible model specification in a rigorous Bayesian statistical framework to incorporate some features, such as uncertainties, concentration dependence, larger numbers of sources, and more than one group of the same species from different sites. The SIAR software package was used to estimate the source proportions that satisfy mass balance, considering three potential carbon sources that could contribute to the food of *Typhlatya* species. SIAR package creates an estimated distribution based on the isotopic data from each source and from each biomass and uses that distribution in the model.

To assess the contribution of different carbon sources to *Typhlatya* species we considered three carbon sources: modern organic matter (OM), modern methanogenic carbon (MM) and ancient methanogenic carbon (AM). The two mixing-model scenarios considered the same OM and MM sources but two different end values for the AM. Biomass values of  $\delta^{13}\text{C}$  and  $\Delta^{14}\text{C}$ , as well as values published for the three potential sources were incorporated into the SIAR software. OM represents a modern carbon pool fixed through photosynthesis by

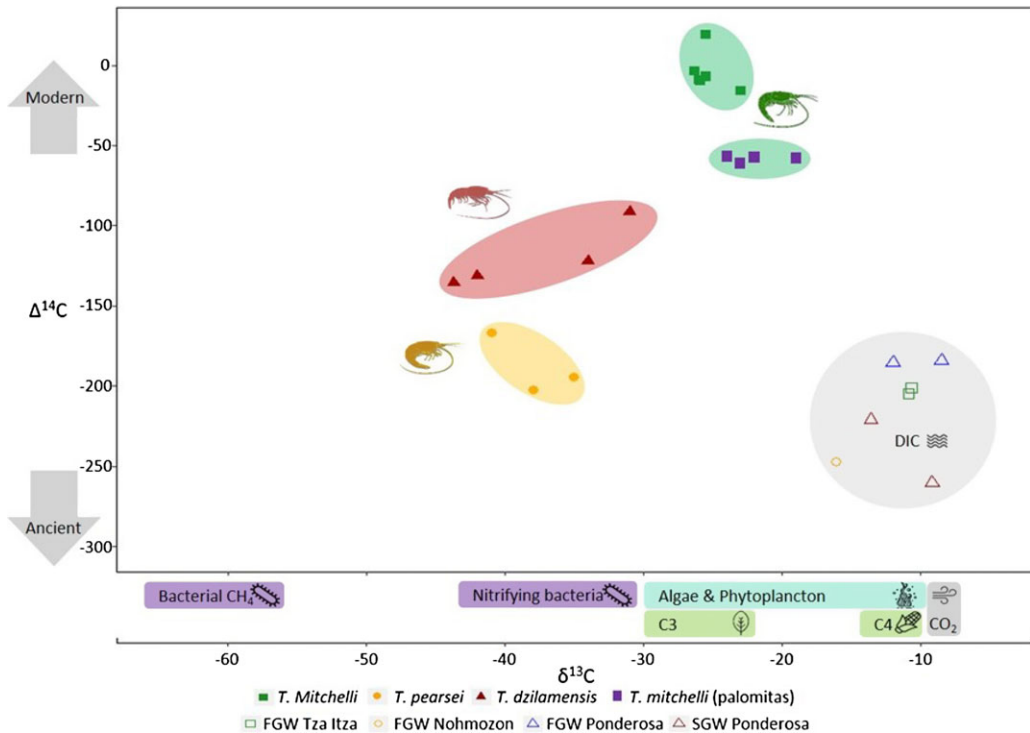


Figure 3 AMS carbon isotopic analysis showing the  $\Delta^{14}\text{C}$  and  $\delta^{13}\text{C}$  composition of *Typhlatya* biomass and dissolved inorganic carbon contained in groundwater. Full symbols represent *Typhlatya* biomass data while void symbols represent groundwater data. Modified from Chávez-Solís et al. (2020).

both aquatic algae and phytoplankton located in the cenote pool and by terrestrial plants in the immediate surroundings. MM represents terrestrial methane produced by fermentation of methylated substrates with a modern signature. AM denotes  $^{14}\text{C}$  depleted sources due to either the methanogenic decomposition of old organic matter by methane oxidizing bacteria (MOB) (scenario 1), or the assimilation of ancient DIC made available through the dissolution of limestone (scenario 2).

## RESULTS AND DISCUSSION

Samples consisted of 4 new and 13 previously published (Chavez-Solís et al. 2020) *Typhlatya* biomass samples (Table 1). Additionally, three new and four previously published (Chavez-Solís et al. 2020) DIC from cenote water samples were analyzed. Carbon composition in *Typhlatya* biomass can be separated into four groups (Figure 3): FGW *T. mitchelli* from Tza Itza, had  $\delta^{13}\text{C}$  values ranging from  $-26.3$  to  $-25.0\text{‰}$ , while *T. mitchelli* from cenote Palomitas (the new sampling site), had a wider and lower range, from  $-24.0$  to  $-19.0\text{‰}$ . The FGW *T. pearsei* from Nohmozon and SGW *T. dzilamensis* from Ponderosa had markedly lower  $\delta^{13}\text{C}$  values ranging from  $-35.0$  to  $-41.0\text{‰}$ , and from  $-31.0$  to  $-44.0\text{‰}$  respectively. The  $\Delta^{14}\text{C}$  values for *T. mitchelli* from Tza Itza varied from  $-3.5$  to  $+19.2\text{‰}$  while the new collected *T. mitchelli* from Palomitas had markedly lower values varying from  $-56.1$  to  $-60.2\text{‰}$ . *T. pearsei* collected in FGW had  $\Delta^{14}\text{C}$  values from  $-202$  to  $-166\text{‰}$ .

*T. dzilamensis* collected in SGW showed  $\Delta^{14}\text{C}$  values from  $-135.5$  to  $-91.5\text{‰}$ . Values of  $\Delta^{14}\text{C}$  from groundwater DIC in all sampled cenotes ranged from  $-185$  to  $-260\text{‰}$ .

The wide range of  $\delta^{13}\text{C}$  and  $\Delta^{14}\text{C}$  values observed in *Typhlatya* collected from FGW and SGW environments, reflect a mixture of modern and ancient carbon contributing to their biomass, as previously suggested for other organisms from anchialine environments (Pohlman 2011).

### Mixing Model Analysis

For OM,  $\delta^{13}\text{C}_{\text{OM}} = -25.4\text{‰}$ , and  $\Delta^{14}\text{C}_{\text{OM}} = -4.3\text{‰}$  values were used in both scenarios. They correspond to the  $\delta^{13}\text{C}$  and  $\Delta^{14}\text{C}$  average values we measured for *T. mitchelli* from Tza Itza (which were the closest to modern carbon). For MM, we used  $\delta^{13}\text{C}_{\text{MM}} = -66.3\text{‰}$  taken from Brankovits et al. (2017), and  $\Delta^{14}\text{C}_{\text{MM}} = -4.3\text{‰}$  for both scenarios. For scenario 1 we used  $\delta^{13}\text{C}_{\text{AM}} = -56.3\text{‰}$  taken from literature Brankovits et al. (2017) and  $\Delta^{14}\text{C}_{\text{AM}} = -1000\text{‰}$  (older than 50,000 BP), and for scenario 2, we considered  $\Delta^{14}\text{C}_{\text{AM}} = -260\text{‰}$ , the most negative value that we measured, that corresponds to the DIC from SGW in Xtabay (Chávez-Solís et al. 2020).

Figure 4 shows the Diagnostic Matrix plot that resulted from the Bayesian model. Analyzed *Typhlatya* are labelled as follows: *T. mitchelli* (labelled group 1 from Tza Itza and group 4 from Palomitas), *T. pearsei* (Group 2) and *T. dzilamensis* (Group 3). The histograms on the diagonal show the relative contribution of each source. The upper triangle shows the contour plots, which indicate how each pair of sources are correlated and the lower triangle indicates the correlation coefficient obtained from the contributions of each source to the diet of each species.

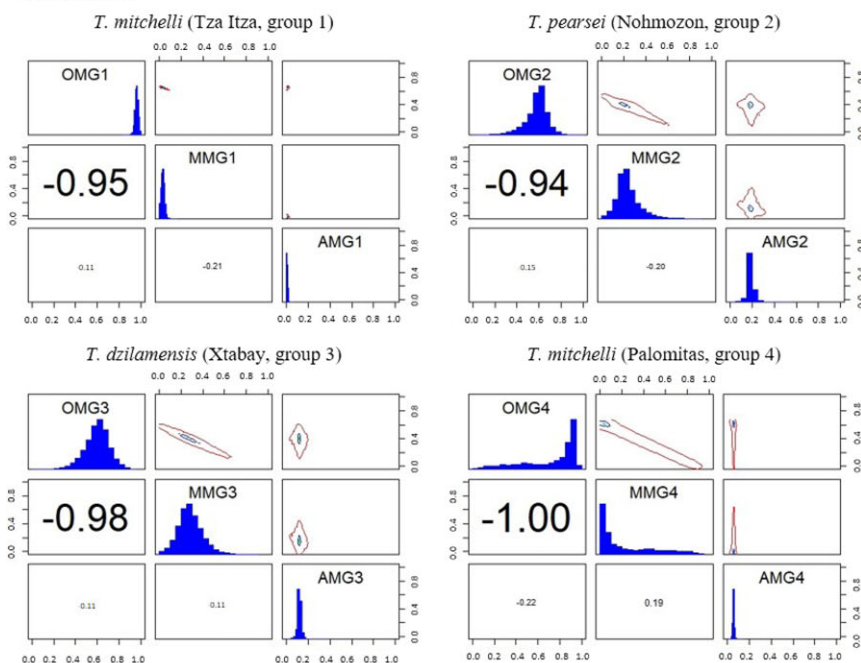
In scenario 1, isotopic signatures of *T. mitchelli* correspond to modern carbon fixed through photosynthesis by both aquatic algae and phytoplankton. The slight differences allow to elucidate that *T. mitchelli* from the two cenotes (groups 1 and 4 of Figure 4) depend on the same carbon sources despite the distance between cenotes and the sampling depth, and both uptake OM in a proportion higher than 90%, while the correlation between OM and MM is narrower for group 1 (Tza Itza) than group 4 (Palomitas). For *T. mitchelli* from Palomitas, it should be noted that its habitat was under a sulfur cloud, which suggests an environment with little organic matter which is reflected in the shape of the surface plots for group 4. These results suggest this population may have modified their diet, feeding almost exclusively on MO, and less MM than what was observed in Tza Itza. The low dispersion observed in the AM histogram suggests that *T. mitchelli* from Palomitas is consuming approximately 20% of AM. These results show that *T. mitchelli* incorporates recently fixed organic carbon independently if it is in surface waters of the cenote pool or greater depths in the cavern.

The results obtained for *T. pearsei* and *T. dzilamensis* characterized by lower  $\delta^{13}\text{C}$  and  $\Delta^{14}\text{C}$  values, indicate that, while *T. mitchelli* carbon originates almost exclusively from a modern source, the later species are partially incorporating carbon from different sources. Both species, *T. pearsei* and *T. dzilamensis* apparently depend to a certain degree on methane chemosynthetically produced from ancient carbon in the interior of the cavern and cave respectively.

The results obtained from scenario 1 indicate that the OM and MM sources are highly correlated (Figure 4). The isotopic composition of these two sources is very similar in their



**Scenario 1**



**Scenario 2**

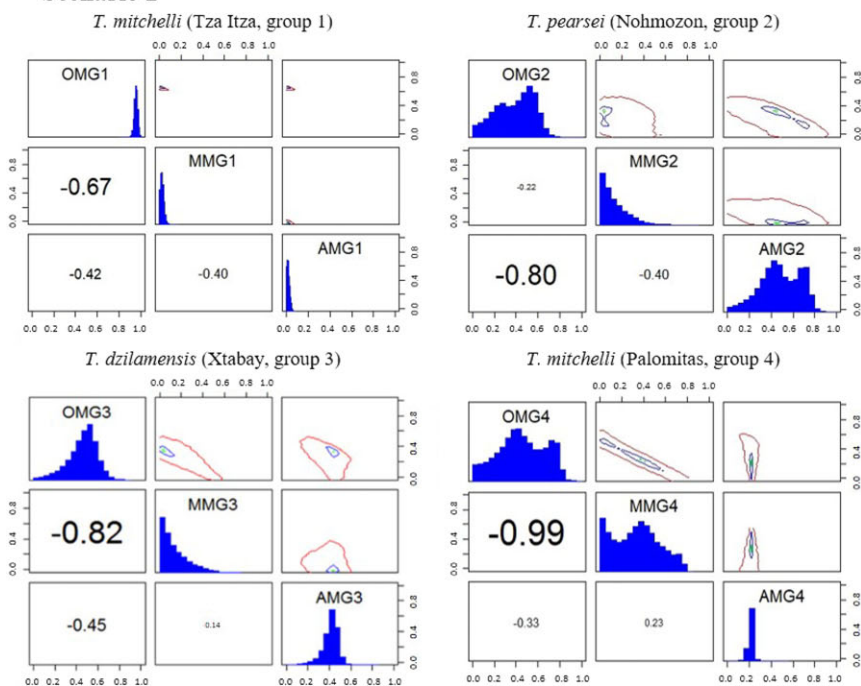


Figure 4 Matrix plots calculated with SIAR for each scenario and source, along with the corresponding correlation factors, and the densities of proportion of each carbon source for each group of *Typhlatya* for scenarios 1 (top) and 2 (bottom). *Typhlatya mitchelli* was collected in site 4 (Group 1) and in site 6 (Group 4); *T. pearsei* was collected in site 5 (Group 2); *T. dzilamensis* was collected in site 7 (Group 3).

posterior distributions, indicating that probable solutions could imply the uptake of one or the other sources, but not simultaneously, as they are inversely correlated and spread out in the surface plots (Figure 4). This implies that when *T. mitchelli* is not consuming MM, it is consuming OM.

For the conditions established in scenario 2, results obtained in this work, corroborate that *T. mitchelli* from Tza Itza (group 1) feed almost exclusively on OM (Chávez-Solís et al. 2020). However, *T. mitchelli* from Palomitas (group 4), collected at 45 m depth, and below the sulfur cloud, acquires AM in a greater proportion than those in Tza Itza (approximately 20%). The presence of a sulfur cloud seems to play an important role in this population, probably related to a greater availability of AM in the Palomitas cenote, in contrast to Tza Itza. Nevertheless, the effects observed in the *T. mitchelli* of Palomitas should not be interpreted as depth dependent, and rather on the availability of OM, MM and AM sources. Regarding *T. pearsei* and *T. dzilamensis*, the results for scenario 2 indicate similar carbon source incorporation, even though they are living in different salinity layers and several hundred kilometers apart.

In summary, in scenario 1, where the AM source is moderately negative and close to  $^{14}\text{C}_{\text{MM}}$  values, the model fails to distinguish between the contributions of OM and MM. On the other hand, when AM is fixed with a lower value, as in scenario 2, the model shows that *T. mitchelli* from Palomitas (group 4) consumes a greater amount of AM. The presence of a sulfur cloud in cenote Palomitas could be related to an anoxic and oligotrophic environment, which could explain why ancient or modern methane incorporation increases its importance for *T. mitchelli* in this particular habitat.

The incorporation of this new data suggests that *T. mitchelli* may have the ability to resort to a greater array of carbon sources than previously suggested (Chávez Solís et al 2020). Ecologically, this could imply that *Typhlatya* species may have a greater feeding plasticity when resources are scarce, and resort to other available feeding sources. Nevertheless, a greater number of individuals from each species and from a greater number of sites would improve our resolution and understanding of the niche breadth of these species, along with the contribution of each source to this abundant and widespread groundwater genus.

## CONCLUSIONS

The local environment exerts a great influence on the isotopic content of the biomass of *Typhlatya*. This suggests that *T. mitchelli* may resort to methanogenic carbon sources in an oligotrophic environment.

Results obtained in this work with Bayesian inference using SIAR (Parnell and Jackson 2013) show similar results as those obtained by Chávez-Solís et al. (2020) using IsoSource mixing model Software (Phillips and Gregg 2003), corroborating the use for this approach in unraveling trophic relations in anchialine systems. The wide range of  $\delta^{13}\text{C}$  and  $\Delta^{14}\text{C}$  values observed in *Typhlatya* species collected from fresh and saline groundwater environments reflect a mixed contribution of photosynthetic and chemosynthetic derived matter, as well as modern and ancient carbon that contributes particularly to the biomass of each species.

## ACKNOWLEDGMENTS

We thank Arcadio Huerta for maintenance and operation of the AMS system and Sergio Martínez for technical assistance. This Project was partially funded by grants from DGAPA PAPIIT IG100619 and CONACyT 315839. We also thank the editor and both anonymous reviewers whose comments and suggestions improved this contribution.

## COMPETING INTERESTS

The authors declare no competing interests.

## REFERENCES

- Benítez S, Iliffe TM, Quiroz-Martínez B, Alvarez F. 2019. How is the anchialine fauna distributed within a cave? A study of the Ox Bel Ha System, Yucatan Peninsula, Mexico. *Subterranean Biology* 31:15–28.
- Brankovits D, Pohlman JW, Niemann H, Leigh B, Leewis MC, Becker KW, Iliffe TM, Alvarez F, Lehmann MF, Phillips B. 2017. Methane-and dissolved organic carbon-fueled microbial loop supports a tropical subterranean estuary ecosystem. *Nature Communications* 8(1):1–3.
- Chávez-Solís, EM, Solís C, Simões N, Mascaró M. 2020. Distribution patterns, carbon sources and niche partitioning in cave shrimps (Atyidae: Typhlatya). *Scientific Reports* 10(1):1–16.
- McCallister L, Bauer J, Cherrier J, Ducklow H. 2004. Assessing sources and ages of organic matter supporting river and estuarine bacterial production: a multiple-isotope ( $\Delta^{14}\text{C}$ ,  $\delta^{13}\text{C}$ , and  $\delta^{15}\text{N}$ ) approach. *Limnology and Oceanography* 49(5):1687–1702.
- Parnell A, Jackson A. 2013. Siar: Stable Isotope Analysis in R (R package version 4.2). <https://cran.r-project.org/package=siar>.
- Phillips D, Gregg J. 2003. Source partitioning using stable isotopes: coping with too many sources. *Oecologia* 136(2):261–269.
- Pohlman JW. 2011. The biogeochemistry of anchialine caves: progress and possibilities. *Hydrobiologia* 677(1):33–51.
- Prasad G, Culp R, Cherkinsky A. 2019.  $\delta^{13}\text{C}$  correction to AMS data: values derived from AMS vs IRMS values. *Nuclear Instruments and Methods in Physics Research B* 455:44–249.
- Stuiver M, Polach H. 1977. Discussion Reporting of  $^{14}\text{C}$  Data. *Radiocarbon* 19(3):355–363.